

Unifying Gompertzian growth with the communicable disease spreading paradigm

Matz Andreas Haugen^{a,*}, Dorothea Gilbert^b

^a*Enerhauggata 1, 0651 Oslo, Norway*

^b*University of Oslo, Oslo, Norway*

Abstract

Recently, a number of studies have shown that cumulative mortality followed a Gompertz curve in the initial Coronavirus epidemic period, March-April 2020. We show that the Gompertz curve is incompatible with the traditional communicable disease spreading hypothesis, and propose a new theory which better explains the nature of the mortality characteristics based on an environmental stressor. Second, we show that for the Gompertz curve to emerge, the stressor has to act on everyone simultaneously, rejecting the possibility of a disease propagation stage. Third, we show that the population acts like a coherent organism under growth/depletion. Finally, we connect the Susceptible-Infected-Recovered (SIR) model with our new theory and show that the SIR model is compatible with Gompertzian growth only when all nodes in the transmission network communicate with infinite speed and interaction.

Keywords: Gompertz, Coherence, Covid, Coronavirus, Network Analysis, Stochastic

1. Introduction

Traditional communicable disease spreading theory assumes a pathogen which infects the population through a network of transmission. Following this line of reasoning it can be theoretically shown that in the early stages of an epi-

*Corresponding author

Email address: matzhaugen@gmail.com (Matz Andreas Haugen)

5 demic, growth follows a logistic-like curve, where the very beginning exhibits exponential growth, and for which analytic and semi-analytic solutions have recently emerged [1, 2, 3, 4]. A large body of research has emerged that explores how these models fit the recent mortality seen due to the Coronavirus epidemic [5, 6, 7, 8, 9, 10].

However, instead of showing logistic-like growth, observed cumulative mortality in the initial period March-April 2020 exhibits almost perfect resemblance to Gompertzian growth [11, 12] where the log-transformed cumulative mortality, or log-mortality for short, is exponentially *decreasing* in time,

$$\frac{d}{dt} \ln Y(t) = -\beta \ln \frac{Y(t)}{\tilde{Y}} + \nu, \quad (1)$$

with constants \tilde{Y} , β , and ν , and whose solution is given as

$$Y(t) = Y_\infty \left(\frac{Y_0}{Y_\infty} \right)^{e^{-\beta t}}, \quad (2)$$

10 where $Y_0 = Y(t=0)$ and $Y_\infty = Y(t \rightarrow \infty) = \tilde{Y} e^{\nu/\beta}$.

This phenomenon is recorded by [13, 14, 15, 16, 17], showing Gompertz curves at national levels instead of the traditionally predicted logistic curves. What is causing such a discrepancy between reality and the current theory of communicable diseases [18]?

One could approach this conundrum from parametrization of the Susceptible-Infected-Recovered (SIR) model under a time-dependent infection/recovery rate ratio, $\phi(t)$ [19]. How would $\phi(t)$ have to behave? Start by recalling the SIR model for a pool of susceptible people of size N evolving between the three states: susceptible, $S(t)$, recovered, $R(t)$ and infected, $I(t)$,

$$\frac{dS}{dt} = -\beta \frac{IS}{N} \quad (3)$$

$$\frac{dI}{dt} = -\beta \frac{IS}{N} - \alpha I. \quad (4)$$

$$\frac{dR}{dt} = \alpha I, \quad (5)$$

15 omitting the argument t in each variable for brevity and where α and β in this context signify recovery and infection rates.

A line of reasoning employed by Rypdal and Rypdal [14] to obtain the Gompertz curve is to linearize the SIR model by assuming both the number of infected, $I(t)$, and cumulative infected, $Y(t)$, is much less than the total population, $N \gg Y \geq I$, which seems well founded at the national level, viz.

$$\frac{dY}{dt} = \beta I \quad (6)$$

$$\frac{dI}{dt} = (\beta - \alpha)I = \alpha(\phi(t) - 1)I, \quad (7)$$

and where the number of recovered, $R(t)$, is under this linearization decoupled from the other variables.

They further assume the number of diseased is proportional to the number of cumulative infected, offset by a time lag, which allows us to use the same set of linearized equations to model the number of cumulative people diseased without loss of generality.

Due to this linearization, the infection/recovery ratio, $\phi(t)$, will have to change as a function of time to accommodate for the boundary conditions. And since I is a function of Y , we can combine (6) via an instantaneous relative growth rate, $\gamma(t) = dY(t)/(Y dt) = \beta I/Y$, in turn parameterized by a scaling factor, θ , representing the shape of the growth,

$$\frac{dY}{dt} = \gamma(t)Y(t) \quad (8a)$$

$$\gamma(t) = \frac{\gamma_\infty}{\theta} \left[1 - \left(\frac{Y}{Y_\infty} \right)^\theta \right], \quad (8b)$$

where $\gamma_\infty = \gamma(t \rightarrow \infty)$. This parametrization is the commonly used Richard's growth curve [20], also called θ -logistic growth, and has been used by others [21]. Although not immediately justified in the communicable disease theory, one could imagine that θ represents non-linear network behavior [22]. Note that at $\theta = 1$, the traditional logistic growth curve is obtained, while at $\theta \rightarrow \infty$ we recover the exponential (Malthusian) explosion.

The observed Gompertzian mortality curves are realized in the limit $\theta \rightarrow 0$,

with the relative growth rate,

$$\gamma(t) = \lim_{\theta \rightarrow 0} \frac{\gamma_\infty}{\theta} \left[1 - \left(\frac{Y}{Y_\infty} \right)^\theta \right] = \gamma_\infty \ln \frac{Y_\infty}{Y} \quad (9)$$

At this limit the growth rate approaches infinity as $Y \rightarrow 0$, which seems
 30 odd under the hypothesis that the pathogen has just started spreading. The
 Gompertzian limit also implies a decreasing relative growth rate from the very
 first time point, which under the SIR model seems unlikely given the large pool
 of susceptible people in the beginning. One would rather expect a near-constant
 relative growth rate in the beginning due to a disease propagation stage. Rypdal
 35 and Rypdal [14] suggest that the decreasing relative growth rate is caused by
 social and political mitigating efforts, but these hardly justify such coherent and
 consistent mortality characteristics across countries.

Perhaps a more likely scenario from which a Gompertz curve would emerge
 is the selective infection of central nodes in the transmission network resulting
 40 in an immediate decrease in relative growth. On the other hand, an infection of
 peripheral nodes should cause immediate exponential growth. Herrmann and
 Schwartz [23] studied a networked SIR model on a variety of networks, but did
 not elaborate on a possible fit to a Gompertz curve. Although it may be possible
 to realize Gompertzian growth from a special network, firm theoretical work has
 45 yet to be done to show this connection. We will touch upon how the Gompertz
 curve emerges from one such network below, under some caveats.

1.1. The SIR model family is almost Gompertzian

Without the linearization and the somewhat arbitrary θ -parametrization,
 one can still obtain from the communicable disease models growth which is
 almost Gompertzian, i.e. a straight line under a double-log transform of (2),
 viz.

$$\ln(\ln(Y_\infty/Y)) = -\beta t + k, \quad (10)$$

with $k = \ln \ln \frac{Y_\infty}{Y_0}$. To show this, we follow Carletti et al. [5] and consider the
 extended version of the SIR the model by including a group of diseased, $D(t)$,

such that $N = S(t) + I(t) + R(t) + D(t)$, also called the SIRD model. This requires an addition to our original set of equations (3), with a extra equation for the diseased group's growth at some rate δ relative to the current infected group,

$$\frac{dD}{dt} = \delta I. \quad (11)$$

Some algebraic manipulations reveal that the diseased group is described by a single equation, viz.

$$\frac{dD}{dt} = \eta(1 - e^{-\xi D}) - \kappa D, \quad (12)$$

where $\eta = \delta N$, $\xi = \beta/(\delta N)$, $\kappa = \delta + \alpha$, and where N is assumed synonymous to the initial susceptible pool of people. This pool of people cannot be obtained
50 from deaths alone, but can be inferred by assuming a known ratio between mortality and recovery, δ and α . When only modeling the diseased however, knowledge of N is irrelevant and the three parameters in (12) are sufficient.

Note here that small values of D follow logistic growth, viz.

$$\frac{dD}{dt} = bD(1 - D/K), \quad (13)$$

obtained with a second order expansion of the exponential term in (12) and with $b = \eta\xi - \kappa$ and $K = 2b/\eta\xi^2$. The SIR and SEIR model exhibits similar properties
55 and its discrepancy with initial observations related to the Coronavirus epidemic has been noted by others [24].

With the full 3-parameter single ODE of the diseased group in the SIRD model, one can obtain a curve quite close to a straight line in the double-log domain even in the initial observations, although there will always be a non-zero concavity (Fig. 1 and Supplemental Information). Meanwhile, even though the Gompertz model can be fit with a 3-parameter model as shown in (1), it can also be simplified to a 2-parameter model estimated through linear regression of log-mortality,

$$\frac{d}{dt} \ln Y(t) = -\beta [\ln Y(t) - \ln Y_\infty]. \quad (14)$$

Thus, through linear regression estimates, the Gompertz model mitigates the possibility of non-identifiability issues of the parameters [25].

Note also that the SIRD model above considers average macroscopic behavior of an ensemble of microscopic units justified through mean-field theory [26] which does not consider network effects explicitly. Rather, all entities are connected and communicating instantaneously as shown by Mombach et al. [27]. However, even with such strong assumptions, it is odd that observed mortality never exhibits a stage of near-exponential growth as this macroscopic SIRD model predicts, but rather a constant negative slope in the double-log domain. We are thus prompted to look for another model which can explain the observed mortality patterns.

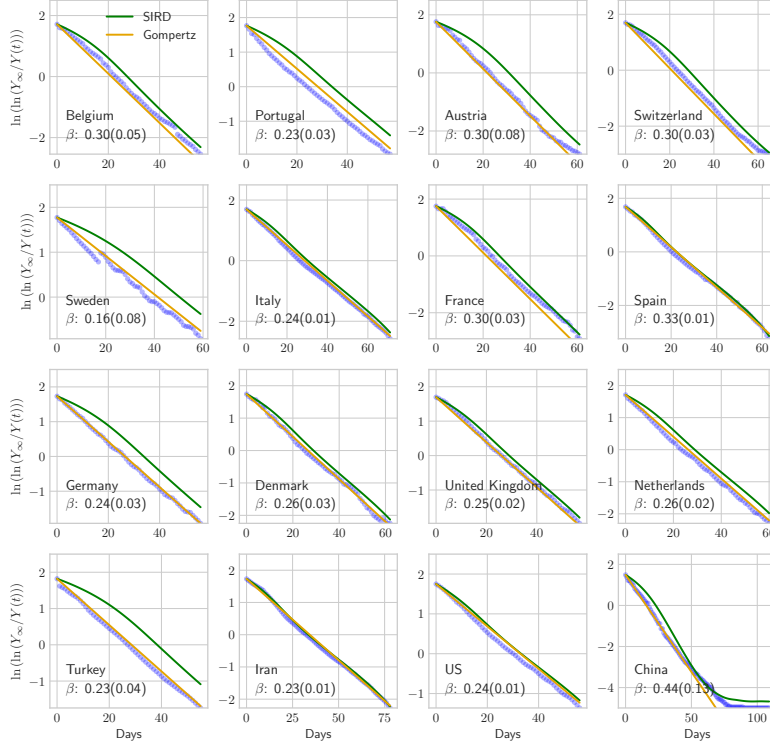


Figure 1: Cumulative number of diseased from the Coronavirus, transformed by $g(Y) = \ln \ln(Y_\infty/Y(t))$ plotted against number of days elapsed after $Y(t)/Y_{max} > 0.005$, comparing a SIRD model with a Gompertz model for a variety of countries in the period Jan-May 2020. Both models are fit using non-linear least squares according to equations (1) and (12) in the text. Although the Gompertz curve can also be obtained with a simple linear fit using (14), it is here obtained using non-linear least squares to put both models on equal footing. The temporal evolution of the SIRD model is obtained from the Runge-Kutta algorithm, while the Gompertz has a closed form for its temporal evolution. Each plot is annotated with an inferred transmission rate in the SIRD model with 1 standard deviation in brackets, assuming bi-normally distributed parameter estimates. Fitting is done with Python-Scipy and a 6-day windowed average of deaths. Observations are taken from the Github repository compiled by the Center for Systems Science and Engineering (CSSE) at Johns Hopkins University, Baltimore, USA [28].

2. An alternative theory for observed mortality

An alternative line of reasoning that does not rely on the framework of communicable diseases is that the biosphere was perturbed by an external stressor, initiating a stress response to eventually bring mortality rates back to stability. This could explain the immediate dampening of mortality growth observed. It could also explain the lack of correlation between population density and mortality (or infection) rates observed by some [29, 30, 31, 32, 33, 34].

Inspired by De Lauro et al. [35], the stressor can be modeled as a multiplicative stochastic dampening term along with a countering force of the immune system. As with all multiplicative processes, it is convenient to log-transform mortality and work in a dimensionless space such that $F(t) = Y(t)/Y_\infty$ and $Z(t) = \ln F(t)$, from which a natural perturbation model emerges,

$$dZ(t) = -\beta Z(t)dt + \sqrt{\sigma}dW(t), \quad (15)$$

where $dW(t)$ is a delta-correlated Wiener process with zero mean, making $Z(t)$ a stochastic process. The first term on the right hand side represents the growth due to the stressor, while the second represents the stress response.

This perturbation model is called an Ornstein–Uhlenbeck process [36]. It is also interpreted as Newton’s equation of motion with friction and a random force (Langevin’s equation), and a continuous version of an Auto-Regressive(1) model [37]. The diffusion coefficient, σ , represents the strength of the perturbation, which we directly see if we recast this equation in terms of mortality while introducing a new parameter $K = \exp(-\frac{\sigma}{2\beta})$, viz.

$$dF(t) = \left\{ \frac{\sigma}{2}F(t) - \beta F(t) \ln \left[\frac{F(t)}{K} \right] \right\} dt + \sqrt{\sigma}F(t)dW(t). \quad (16)$$

To obtain the deterministic observable, we first take the average in the log-domain (15) and transform back to the original domain,

$$d\langle \ln F(t) \rangle = -\beta \langle \ln F(t) \rangle dt, \quad (17)$$

where the bra-ket notation signifies the averaging operation. Then we use the

property that the average of log-quantities is the logarithm of the median quantity, where we denote the median of $F(t)$ as $M(t)$,

$$d \ln M(t) = -\beta \ln M(t) dt, \quad (18)$$

which corresponds with the familiar deterministic Gompertz differential equation in (1) with $Y(t) = Y_\infty M(t)$. Comparing the stochastic stressor σ in 16 with the deterministic growth equation in (1) gives $\nu = \sigma/2$, suggesting that the stressor is indeed the source of growth, while β is the growth-limiting factor. We also see that by comparing (8a) and (9) with the stochastic counterpart in (16) that the final growth level is governed by the stressor magnitude,

$$\sigma = 2\gamma_\infty \ln Y_\infty. \quad (19)$$

Thus, a more parsimonious interpretation of the observations not reliant on a transmission network is that mortality was caused by a planetary perturbation, modeled as a random process, to which organisms gradually develop resistance at a geometric rate in the log-transformed domain [38, 39], which is the natural transformation for many processes in nature [40]. Under this model, the distribution of the abundance of $F(t)$ is log-normal, a result that can be obtained by directly solving the stochastic equation in (16) [41, 42], or from thermodynamic principles [43, 44, 45]. Intuitively, this is seen by noting that the solution to the perturbation model in the log-domain (15) is Gaussian in the variable $Z(t)$, thus suggesting a log-normal distribution of $F(t)$. This implies that the log-domain is the domain in which the central limit theorem applies.

3. Unifying the SIR model and the Gompertz model

This remarkable observation that the log-transformed domain is the natural one merits closer study. First, juxtapose the logistic model with the Gompertz model,

$$\dot{M} = \frac{d}{dt}M(t) = \beta M(t)(1 - M(t)) \quad \text{Logistic} \quad (20a)$$

$$\frac{d}{dt} \ln(M(t)) = -\beta \ln(M(t)) \quad \text{Gompertz}, \quad (20b)$$

where $M(t)$ is deterministic.

In the logistic model, we recognize the rightmost side of the logistic equation
 95 as the transmission term in an SIR model, but also as a linear interaction term between the two macroscopic states. As mentioned earlier, this procedure is a mean field approximation with an implied average interaction between the variables. Thus, all dynamics are governed by macroscopic deterministic variables parametrized by a transmission rate.

A microscopic solution could be modeled by splitting the system into N microscopic deterministic units, $M(t) \rightarrow x_1(t), x_2(t), \dots, x_N(t)$, where the lower case x_i emphasizes the microscopic quality of the variables, and is here interpreted as probability of infection. From these microscopic units, macroscopic growth could be obtained by taking their arithmetic average,

$$M(t) = \frac{1}{N} \sum_i^N x_i(t). \quad (21)$$

100 Naturally, this simple arithmetic average treats each microscopic unit as independent variables contributing to the macroscopic observable.

One could add network interaction necessitating a corresponding matrix version of (20a)

$$\frac{dx_i}{dt} = \beta(1 - x_i) \sum_j a_{ij} x_j \quad \forall i, \quad (22)$$

using the shorthanded $x_i = x_i(t)$ and with a fixed correlation governed by the network's growth rate, β , and adjacency matrix, $\{a_{i,j}\} = \mathbf{A} \in \mathbb{R}^{N \times N}$, a binary matrix with ones where the i^{th} and j^{th} nodes are connected, and zeroes otherwise. Notice here that there is an implied causality going from the infected to susceptible, which will become relevant below. Furthermore, a linear correlation between variables is seen as the partial derivatives of the

instantaneous growth rate with respect to pairs of microscopic variables,

$$\frac{\partial^2 \dot{M}}{\partial x_i \partial x_j} = -\frac{\beta}{N} a_{i,j}. \quad (23)$$

Still, no Gompertz curve will emerge at the onset of the growth process. Estrada and Bartesaghi [46] provide illuminating analysis on this topic.

In contrast, as discussed in Section 2, the Gompertz model is implied by a
105 multiplicative stochastic process with a log-normal distribution in its abundance at any given point in time. As mentioned earlier, this implies that the log-domain is the natural domain in which the central limit theorem applies, thus implying correlated mortality growth through the geometric mean,

$$M(t) = \exp \left[\frac{1}{N} \sum_i \ln x_i(t) \right] = \left[\prod_i x_i(t) \right]^{\frac{1}{N}} \quad (24)$$

Under this model, correlation between entities is present at all orders in the
110 original domain and all the nodes in the network communicate instantaneously¹.

Thus, the emergence of the Gompertz curve at the macroscopic level suggests that the system is correlated, or coherent, presumably as a result of the simultaneous exposure to the same underlying stressor, but also due to the implied log-normal nature of the microscopic entities, where multiplication re-
115 places addition as the aggregating operator [40]. We can now further appreciate Richard’s parametrization as a transition from non-collaborative to collaborative growth as $\theta \rightarrow 0$. This feature of θ was also obtained by Petroni et al. [22] by interpreting the θ -logistic growth rate in (8) as non-linear resource availability dependent on the overall magnitude, $Y(t)$, with growth at $\theta \rightarrow 0$
120 named “maximally coherent”. Molski and Konarski [48] made a similar observation that Gompertzian growth is the coherent state in a quantum mechanical

¹It is illuminating to at this point compare with Gompertz’ Law of Mortality, $\frac{d}{dt} \ln(1 - M(t)) = -\beta$, for t more than 25 years, which yields a naturally uncorrelated macroscopic curve $1 - M(t) = \exp(-\beta t)$ [47]. In our context, the uncorrelated feature emerges since the force of mortality is not a function of the growth itself, as we see in the text, but rather of time.

system with a time-dependent potential, an interpretation which sheds further light on the temporal nature of the postulated stress response. This quantum mechanical system has also been used to describe coherent energy states of di-
125 atomic molecules in space [49]. In the field of quantum physics, *coherence* is a well-defined mathematical property first explored by Glauber [50] in the context of electromagnetic fields. The fact that we observe the Gompertz curve in both the microscopic quantum scales and the macroscopic national scales is quite noteworthy. It suggests that both systems share commonalities and means of
130 communication.

3.1. Unification through a modified SIR model

However, it is possible to reconcile the SIR model with the Gompertz curve. Inspired by the observation that in the linearized approximation there are only two coupled states, infected and susceptible, we augment the interaction term to higher orders. Then, we reverse the causality where the population of infected are now dependent on the population of the susceptible instead of the other way around as in (22),

$$\frac{dx_i}{dt} = \beta x_i \sum_j a_{ij} (1 - x_j) \quad \forall i. \quad (25)$$

This crucial change is based on the environmental stressor hypothesis rather than a communicable disease assumption. Furthermore, we will for the sake of simplicity assume all nodes in the network have exactly one neighbor and that there exists a unique path between all nodes,

$$\sum_i a_{ij} = 1 \quad \forall j. \quad (26)$$

If we let $s_i = 1 - x_i$ be the probability of being susceptible, the augmented and causality-reversed SIR model infection term becomes

$$\frac{dx_i}{dt} = \beta x_i \sum_j a_{ij} (s_j + s_j^2/2 + \dots) - \alpha x_i \quad \forall i, \quad (27)$$

Now use the Taylor series $s + s^2/2 + \dots = -\ln(1 - s)$, viz.

$$\frac{dx_i}{dt} = -\beta x_i \sum_j a_{ij} \ln(1 - s_j) - \alpha = -\beta x_i \sum_j a_{ij} \ln x_j - \alpha x_i \quad \forall i, \quad (28)$$

As we are interested in the aggregate macroscopic behavior, we take averages in the log domain, exploit our setup where \mathbf{A} is a single mapping from one node to another, and simplify to

$$\frac{d}{dt} \ln \left[\prod_i x_i \right]^{\frac{1}{N}} = -\beta \ln \left[\prod_i x_i \right]^{\frac{1}{N}} - \alpha. \quad (29)$$

If $\alpha \rightarrow 0$, then this equation will exhibit Gompertzian growth in the geometric ensemble average of microscopic units. An interpretation of $\alpha \rightarrow 0$ could be that the limiting factor emerges purely from the growth rate without the need for a second growth-limiting parameter, in line with the previous crucial hypothesis of causality reversal stated above. One further simplification could be seen in equating the logarithm of the geometric mean with the logarithm of the median of the set of x_i to obtain (18),

$$\frac{d}{dt} \ln M(t) = -\beta \ln M(t). \quad (30)$$

4. Conclusion

In conclusion, we have shown that Gompertzian growth follows from infinite
135 interactions between the susceptible and infected states, and that the perceived pathogen travels at infinite speed throughout the population, rejecting the possibility of a disease propagation stage through a perceived transmission network. In this vein, Richard's parameter, θ , in his growth model paradigm can be related to the number of higher order interactions with the susceptible and the
140 infected in an SIR model [20], where infinite interactions corresponds to $\theta \rightarrow 0$.

We further show that the observed mortality across countries can be explained by a model where the biological system is stressed by a ubiquitous and simultaneous stressor eliciting a corresponding stress response through which gradual return to pre-epidemic conditions are mediated. The stressor is modeled as a stochastic perturbation in the log-transformed domain of effects where
145

correlation between people or microscopic entities is present at all orders. From this model, we draw parallels between the coherent behavior of the population's mortality evolution during an epidemic and the spatial coherence of quantum mechanical systems, borrowing the definition of coherence from quantum physics [48].

Thus, we see growth on a spectrum: In one extreme we find non-collaborative growth models or models with parameterized linear interaction effects, and in the other extreme we see a field of microscopic entities coherently sharing information much like quantum entangled particles. The emergence of coherent quantum phenomena at the macroscopic level suggests that no longer can the microscopic world claim a monopoly on quantum physics, especially as it relates to biology [51]. One might be surprised to find that temporal evolution of human mortality during epidemics can behave like the spatial energy distribution of quantum coherent systems.

Methods

4.1. Estimating model parameters

The time-evolution of the SIRD and the Gompertz model are obtained with a Runge-Kutta algorithm, after first fitting parameters using non-linear least squares according to equations (1) and (12) in the text (Fig. 2). Fitting is done with Python-Scipy with specified Jacobians and a 6-day windowed average of observed deaths. Observations are taken from the Github repository compiled by the Center for Systems Science and Engineering (CSSE) at Johns Hopkins University, Baltimore, USA [28].

The transmission rate is modeled as the product of $\eta\xi$ in (12), and its associated variance is obtained assuming a bi-normal relationship between the two parameters with cross-correlation ρ [52],

$$\text{Var}[\beta] = \text{Var}[\eta]\text{Var}[\xi](1 + \rho^2) + \text{Var}[\xi] * \eta^2 + \text{Var}[\eta]\xi^2. \quad (31)$$

4.2. Code Availability

¹⁷⁰ The computer code required to produce the results are given in the following Github repository,

`https://github.com/matzhaugen/GompertzManuscript`

Supplement

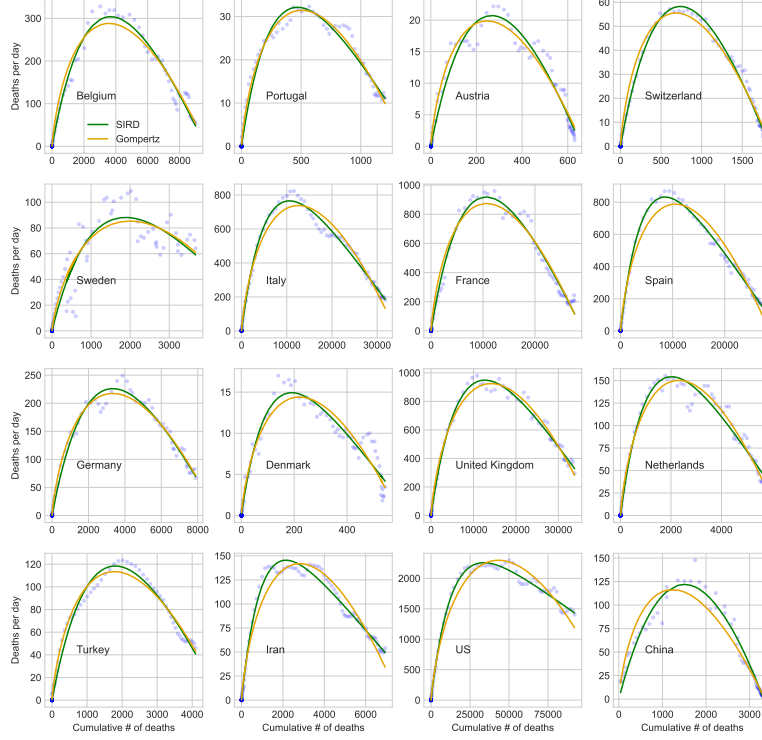


Figure 2: Cumulative diseased plotted against number of days after $Y(t)/Y_{max} > 0.005$, comparing an SIRD with a Gompertz model. Both models are fit using non-linear least squares according to equations (1) and (12) in the text. Fitting is done with Python-Scipy and a 6-day windowed average of deaths. Observations are taken from the Github repository compiled by the Center for Systems Science and Engineering (CSSE) at Johns Hopkins University, Baltimore, USA [28].

Table 1: Estimated values for the SIRD model fitted to various countries' observations as shown in Figure 1 using notation from 12. Standard deviation is given in the paranthesis corresponding to the last significant digit of the reported number.

	$\eta \times 10^{-1}$	$\xi \times 10^4$	$\kappa \times 10^2$
Belgium	94(8)	3.2(2)	9.3(7)
Portugal	6.6(4)	35(2)	4.5(3)
Austria	8(1)	36(5)	11(1)
Switzerland	22(1)	13.6(7)	11.0(5)
Sweden	19(5)	8(2)	3(1)
Italy	137(3)	1.77(5)	3.71(1)
France	240(10)	1.24(7)	8.1(4)
Spain	145(2)	2.27(5)	4.75(8)
Germany	61(4)	3.9(3)	6.5(5)
Denmark	2.7(2)	96(8)	4.3(3)
United Kingdom	181(5)	1.39(5)	4.3(1)
Netherlands	29(1)	8.9(5)	4.3(2)
Turkey	34(3)	6.8(5)	6.9(6)
Iran	22.3(4)	10.4(4)	2.51(7)
US	312(5)	0.76(2)	1.83(7)
China	130(30)	3.5(5)	26(4)

Table 2: Estimated values for the Gompertz model fitted to various countries' observations, as shown in Figure 1 using notation from 1. Standard deviation estimates is given in the paranthesis corresponding to the last significant digit of the reported number.

	$\nu \times 10$	$\beta \times 10^2$	$\tilde{Y} \times 10^2$
Belgium	9.3(1)	8.1(2)	10.1(9)
Portugal	6.15(3)	6.22(7)	7.0(3)
Austria	7.28(7)	8.1(2)	8.1(7)
Switzerland	8.08(6)	8.1(1)	8.9(5)
Sweden	4.9(1)	4.3(2)	6(1)
Italy	7.60(6)	5.88(7)	8.4(4)
France	10.2(1)	8.2(1)	11.0(8)
Spain	9.41(9)	7.5(1)	10.2(7)
Germany	7.56(6)	6.53(8)	8.4(4)
Denmark	5.94(7)	6.5(2)	6.8(7)
United Kingdom	8.46(5)	6.54(7)	9.3(4)
Netherlands	7.34(6)	6.52(8)	8.2(4)
Turkey	7.04(5)	6.38(8)	7.9(4)
Iran	5.87(6)	5.04(8)	6.7(4)
US	7.53(7)	5.32(7)	8.4(5)
China	9.8(1)	9.4(2)	10(1)

References

- 175 1. Harko T, Lobo FS, Mak M. Exact analytical solutions of the susceptible-infected-recovered (sir) epidemic model and of the sir model with equal death and birth rates. *Applied Mathematics and Computation* 2014;236:184–94.
2. Kröger M, Schlickeiser R. Analytical solution of the sir-model for the temporal evolution of epidemics. part a: time-independent reproduction factor.
180 *Journal of Physics A: Mathematical and Theoretical* 2020;53(50):505601.

3. Schlickeiser R, Kröger M. Analytical solution of the sir-model for the temporal evolution of epidemics: part b. semi-time case. *Journal of Physics A: Mathematical and Theoretical* 2021;54(17):175601.
- 185 4. Heng K, Althaus CL. The approximately universal shapes of epidemic curves in the susceptible-exposed-infectious-recovered (seir) model. *Scientific Reports* 2020;10(1):1–6.
5. Carletti T, Fanelli D, Piazza F. Covid-19: The unreasonable effectiveness of simple models. *Chaos, Solitons & Fractals: X* 2020;5:100034.
- 190 6. Cooper I, Mondal A, Antonopoulos CG. A sir model assumption for the spread of covid-19 in different communities. *Chaos, Solitons & Fractals* 2020;139:110057.
7. Postnikov EB. Estimation of covid-19 dynamics “on a back-of-envelope”: Does the simplest sir model provide quantitative parameters and predictions? *Chaos, Solitons & Fractals* 2020;135:109841.
- 195 8. Muñoz-Fernández GA, Seoane JM, Seoane-Sepúlveda JB. A sir-type model describing the successive waves of covid-19. *Chaos, Solitons & Fractals* 2021;144:110682.
9. Cooper I, Mondal A, Antonopoulos CG, Mishra A. Dynamical analysis of the infection status in diverse communities due to covid-19 using a modified sir model. *Nonlinear Dynamics* 2022;:1–14.
- 200 10. Saikia D, Bora K, Bora MP. Covid-19 outbreak in india: an seir model-based analysis. *Nonlinear Dynamics* 2021;104(4):4727–51.
- 205 11. Gompertz B. XXIV. on the nature of the function expressive of the law of human mortality, and on a new mode of determining the value of life contingencies. in a letter to francis baily, esq. f. r. s. &c. *Philosophical Transactions of the Royal Society of London* 1825;115:513–83. doi:10.1098/rstl.1825.0026.

12. Bajzer Ž, Vuk-Pavlović S, Huzak M. Mathematical modeling of tumor growth kinetics. In: *A survey of models for tumor-immune system dynamics*. Springer; 1997:89–133.
13. Ohnishi A, Namekawa Y, Fukui T. Universality in COVID-19 spread in view of the gompertz function. *Progress of Theoretical and Experimental Physics* 2020;2020(12). doi:10.1093/ptep/ptaa148.
14. Rypdal K, Rypdal M. A parsimonious description and cross-country analysis of COVID-19 epidemic curves. *International Journal of Environmental Research and Public Health* 2020;17(18):6487. doi:10.3390/ijerph17186487.
15. Català M, Alonso S, Alvarez-Lacalle E, López D, Cardona PJ, Prats C. Empirical model for short-time prediction of COVID-19 spreading. *PLOS Computational Biology* 2020;16(12):e1008431. doi:10.1371/journal.pcbi.1008431.
16. Rodrigues T, Helene O. Monte carlo approach to model covid-19 deaths and infections using gompertz functions. *Physical Review Research* 2020;2(4):043381.
17. Levitt M, Scaiewicz A, Zonta F. Predicting the trajectory of any COVID19 epidemic from the best straight line 2020;doi:10.1101/2020.06.26.20140814.
18. Castro M, Ares S, Cuesta JA, Manrubia S. The turning point and end of an expanding epidemic cannot be precisely forecast. *Proceedings of the National Academy of Sciences* 2020;117(42):26190–6.
19. Kermack WO, McKendrick AG. A contribution to the mathematical theory of epidemics. *Proceedings of the royal society of london Series A, Containing papers of a mathematical and physical character* 1927;115(772):700–21.
20. Richards F. A flexible growth function for empirical use. *Journal of experimental Botany* 1959;10(2):290–301.

21. Wu K, Darcet D, Wang Q, Sornette D. Generalized logistic growth modeling of the covid-19 outbreak: comparing the dynamics in the 29 provinces in china and in the rest of the world. *Nonlinear dynamics* 2020;101(3):1561–81.
240
22. Petroni NC, De Martino S, De Siena S. Logistic and θ -logistic models in population dynamics: General analysis and exact results. *Journal of Physics A: Mathematical and Theoretical* 2020;53(44):445005.
23. Herrmann HA, Schwartz JM. Why covid-19 models should incorporate the network of social interactions. *Physical Biology* 2020;17(6):065008.
245
24. Vattay G. Forecasting the outcome and estimating the epidemic model parameters from the fatality time series in covid-19 outbreaks. *Physical Biology* 2020;17(6):065002.
25. Roda WC, Varughese MB, Han D, Li MY. Why is it difficult to accurately predict the covid-19 epidemic? *Infectious disease modelling* 2020;5:271–81.
250
26. Smilkov D, Hidalgo CA, Kocarev L. Beyond network structure: How heterogeneous susceptibility modulates the spread of epidemics. *Scientific reports* 2014;4(1):1–7.
27. Mombach JC, Lemke N, Bodmann BE, Idiart MAP. A mean-field theory of cellular growth. *EPL (Europhysics Letters)* 2002;59(6):923.
255
28. Dong E, Du H, Gardner L. An interactive web-based dashboard to track covid-19 in real time. *The Lancet infectious diseases* 2020;20(5):533–4.
29. Hamidi S, Sabouri S, Ewing R. Does density aggravate the COVID-19 pandemic? *Journal of the American Planning Association* 2020;86(4):495–509. doi:10.1080/01944363.2020.1777891.
260
30. Hamidi S, Ewing R, Sabouri S. Longitudinal analyses of the relationship between development density and the COVID-19 morbidity and mortality rates: Early evidence from 1,165 metropolitan counties in the united

- states. *Health & Place* 2020;64:102378. doi:10.1016/j.healthplace.2020.102378.
- 265 2020.102378.
31. Carozzi F. Urban density and covid-19. *SSRN Electronic Journal* 2020;doi:10.2139/ssrn.3643204.
 32. Arpino B, Bordone V, Pasqualini M. No clear association emerges between intergenerational relationships and COVID-19 fatality rates from
270 macro-level analyses. *Proceedings of the National Academy of Sciences* 2020;117(32):19116–21. doi:10.1073/pnas.2008581117.
 33. Khavarian-Garmsir AR, Sharifi A, Moradpour N. Are high-density districts more vulnerable to the covid-19 pandemic? *Sustainable Cities and Society* 2021;70:102911.
 - 275 34. Barak N, Sommer U, Mualam N. Urban attributes and the spread of covid-19: The effects of density, compliance and socio-political factors in israel. *Science of the Total Environment* 2021;793:148626.
 35. De Lauro E, De Martino S, De Siena S, Giorno V. Stochastic roots of growth phenomena. *Physica A: Statistical Mechanics and its Applications*
280 2014;401:207–13.
 36. Risken H. The Fokker-Planck Equation. Springer; 1996.
 37. Akaike H. Statistical predictor identification. *Annals of the institute of Statistical Mathematics* 1970;22(1):203–17.
 38. Boxenbaum H. Hypotheses on mammalian aging, toxicity, and longevity
285 hormesis: Explication by a generalized gompertz function. In: *Biological Effects of Low Level Exposures to Chemicals and Radiation*. CRC Press; 2017:1–39.
 39. Neafsey PJ, Boxenbaum H, Ciraulo DA, Fournier DJ. A gompertz age-specific mortality rate model of aging, hormesis, and toxicity: Fixed-dose
290 studies. *Drug metabolism reviews* 1988;19(3-4):369–401.

40. Zhang CL, Popp FA. Log-normal distribution of physiological parameters and the coherence of biological systems. *Medical Hypotheses* 1994;43(1):11–6.
41. Skiadas CH. Exact solutions of stochastic differential equations: Gompertz, generalized logistic and revised exponential. *Methodology and Computing in Applied Probability* 2010;12(2):261–70.
42. Petroni NC, De Martino S, De Siena S. Gompertz and logistic stochastic dynamics: Advances in an ongoing quest. *arXiv preprint arXiv:200206409* 2020;.
43. Sitaram B, Varma V. Statistical mechanics of the gompertz model of interacting species. *Journal of theoretical biology* 1984;110(2):253–6.
44. Gunasekaran N, Pande L. Log normal distribution for the intrinsic abundance of species from the gompertz model. *Journal of Theoretical Biology* 1982;98(2):301–5.
45. Chakrabarti C, Bhadra S. Non equilibrium thermodynamics and stochastics of gompertzian growth. *J Biol Systems* 1996;4(2):151–7. doi:doi.org/10.1142/S0218339096000119.
46. Estrada E, Bartesaghi P. From networked sis model to the gompertz function. *Applied Mathematics and Computation* 2022;419:126882.
47. Shklovskii B. A simple derivation of the gompertz law for human mortality. *Theory in Biosciences* 2005;123(4):431–3.
48. Molski M, Konarski J. Coherent states of gompertzian growth. *Physical review E* 2003;68(2):021916.
49. Morse PM. Diatomic molecules according to the wave mechanics. ii. vibrational levels. *Physical review* 1929;34(1):57.
50. Glauber RJ. Coherent and incoherent states of the radiation field. *Physical Review* 1963;131(6):2766.

51. Lambert N, Chen YN, Cheng YC, Li CM, Chen GY, Nori F. Quantum biology. *Nature Physics* 2013;9(1):10–8.
- 320 52. Nadarajah S, Pogány TK. On the distribution of the product of correlated normal random variables. *Comptes Rendus Mathématique* 2016;354(2):201–4.